THE EFFECT OF PIPE INSTALLATION ON THE DYNAMIC CHARACTERISTICS OF VARIABLE-DISPLACEMENT AXAIL PISTON PUMP

Yehia EL-MASHAD

Associate Professor, Shoubra Faculty of Engineering

تاثير تركيب الأنابيب على الخواص الديناميكية لمضخة بمكبس محوري متغير الإزاحة

الملخص العربى

عند الغلق المفاجئ لصمام مركب على خط سريان يتم تحويل طاقة الحركة للمائع إلى طاقة انفعال. ونظرا لوجود بعض المرونة بدرجات متفاوتة في هذه الأنابيب فإنها تمتص بعض هذه الطاقة الموجودة بالسائل وتعتمد كمية الطاقة الممتصة على نوع المادة المصنوع منها الأنبوب وكذلك القطر والطول. في هذا البحث تناولنا بالتفصيل تأثير اختيار انابيب ذات مواد وأبعاد مختلفة على الخواص الديناميكية لمضخة محورية ذات إزاحه متغيرة في حالتين للتحميل (زيادة ونقصان خطوة) تم محاكاة مادتين صلبتين مختلفتين ومادتين غير معدنيتين مختلفتين ذات أقطار وأطوال مختلفة. ولقد أوضحت النتائج ضرورة إعطاء أهمية كبيرة لاختيار الأنبوب (مواسير أو خراطيم) وكذلك تحديد نصف القطر والطول المناسب لتأثير ذلك على أداء المنظومة ولتجنب الأداء الغير مرغوب فيه خاصة في التطبيقات الحرجة مثل التحكم في أسطح التحكم وانزال العجلات في الطائرات حيث تكون أطوال المواسير / الخراطيم كبيرة وتؤثر على سرعة الاستجابة ومعدل التخميد.

ABSTRACT

Thc sudden or instantaneous closure of a valve fitted with a pipeline, causes the conversion of kinetic energy of the fluid into strain energy. As every pipe possesses some elasticity, so it absorbs some strain energy along with the fluid, the amount of energy absorption depends on material, diameter and the length of the pipeline. The effect of pipeline material and dimensions on the dynamic characteristics of variable-displacement axial piston pump in two load cases (step decrease and increase load flow) is discussed in some detail. Two different hard materials and two different non metallic materials with different diameters and lengths are simulated. The performance characteristics of the system under these conditions are investigated. The results show the importance of giving great attention to the selection of the pipe installation on the whole performance of the system.

Accepted May 4, 2003.

KEY WORDS

Axial Piston Pump - Power Hydraulic - Dynamics – Control-Pipes and Hoses.

NOMENCLATURE

A_c	Area of pressure compensator spool
A_1	Area of yoke control piston
A_2	Area of pumping piston
A_3	Area of bias yoke control piston
B	Viscous friction coefficient of yoke control piston
C_d	Discharge coefficient of orifice
C_1	Leakage cocfficient of yoke control cylinder
C_2	Leakage coefficient of pump
d	Pipe internal diameter
d_1	Distance form yoke pivot to yoke control cylinder
d_2	Distance form piston slipper joint axis to yoke pivot
d_3	Distance form yoke pivot to bias cylinder
E	Modulus of elasticity
e	Eccentricity of yoke pivot with respect to barrel's axis
g_1	Area gradient of orifice of pressure compensator
g_2	Area gradient of orifice of load control valve
J	Moment of inertia of yoke with respect to yoke pivot
K_1	Coefficient of spring to actuate yoke
K_2	Coefficient of spring to retract the pumping piston during the suction stroke
K_3	Coefficient of spring to determine the desired supply pressure
L	Pressure pipe length
M	Mass of pumping piston
N	Number of pumping pistons
ν	Poisson's ratio
P_d	Distributed pressure around valve plate
P_0	Pressure at suction port of pump
P_p	Pressure in yoke control cylinder
P_s	Outlet pressures of pump or supply pressure to load
P_{sd}	Desired value of the outlet pressure
Q_l	Load flow rate of load control valve
Q_p	Control flow rate of pressure compensator
Q_{lp}	Leakage flow rate from outlet port volume due to control flow rate compensator
R_1	Radius from barrel's axis to pumping pistons
T_t	Total torque on yoke due to inertia force of pumping pistons and pressure force on valve plate
t	Pipe wall thickness
V_0	Volume of yoke control cylinder at yoke angle 'θ=0', radian
V_s	Total pressurized volume of pump and pipeline
x_c	Displacement of spool of pressure compensator
x_l	Displacement of spool of load control valve

GREEK SYMBOLS

α	α- parameter vector
α_1	Flow gain of pressure compensator

α_2	Moment of inertia of yoke (J)
α_3	Viscous friction coefficient of yoke control piston (B)
α_4	Equivalent coefficient of angular spring to actuate yoke
α_5	Initial compression of yoke control spring (θ_o)
α_6	Volumetric displacement of yoke control cylinder
α_7	Equivalent torque coefficient with respect to unit change of outlet pressure
α_8	Leakage coefficient of yoke control cylinder (C_1)
α_9	Oil compliance of yoke control cylinder
α_{10}	Specific displacement of pump
α_{11}	Oil compliance of pipeline
α_{12}	Leakage coefficient of pump (C_2)
α_{13}	Coefficient of torque (T) with respect to displacement of yoke
β	Equivalent bulk modulus of fluid
ρ	Density of fluid
θ	Yoke angle
θ_o	Initial angular compression of spring of yoke motion at yoke angle θ, rad
ϕ	Angular position of barrel-pumping piston
ω	Angular velocity of pump shaft

The units for these coefficients are given later with their simulated numerical values.

1-Introduction

Variable-displacement axial piston pumps are widely used as a power supply in hydraulic systems of many aircrafts, as well as in many industrial and agricultural applications. These pumps can transmit large specific power and their flow rate can be varied. The commonly used types of axial piston pumps can be classified, according to the controlling method, as pressure-compensated control by pilot operation, and flow control by manual operation or auxiliary servo control. The first type has generally a wider range of applications, the other type can be considered in the same way as pressure-compensated type except for the control method. The energy loss of the variable displacement pump is also less than that of the fixed displacement pump with a relief valve. Several investigators like Johnston, et al.[1], Edge, K. A. et al. [2], Kim, S. D. [3], Ye R. Z. [4] Zeiger, G. and Akers [5] have done research about the dynamic properties of a variable displacement piston pump.

Most of these investigations are based on a linearized model of the pump dynamics. In industrial applications, because the dynamic characteristics of the variable delivery pump are always complex and highly nonlinear, Kim [3] studied the dynamic characteristics for the variation of the system parameter values on a non-linear model of the pump dynamics and made a systematic approach to analyze the effect of the system parameters.

The knowledge of static and dynamic characteristics of these pumps is of profound importance in designing sophisticated hydraulic control systems. This is so because the change from an operating condition to another must be done in the soonest possible time and if possible without any oscillations [6].

All of the above researches didn't take into consideration the effect of pipe installation (with its strain energy absorption) on the pump dynamic characteristics especially when the valve is suddenly closed. So in this paper we will study the effect of pipeline material and dimensions on the dynamic characteristics of PVB series pump, the geometrical data and dynamic data of the pump system are shown in Table 1. Two different hard materials with different out-side diameters and lengths (Stainless steel and Aluminum alloy) are used as a tube.

Also two different non-metallic materials with different out-side diameters and lengths (Plastic and Reinforced plastic) are used as a hose in most pump applications. The types, diameters and lengths of the pipelines are shown in Table 2.

2-Mathematical Model and Specifications of the Pump

The structure of the variable displacement axial piston pump is shown in Figure 1; the pilot-operated control of the pressure compensator regulates the outlet pressure and flow to the pre-set values. The exact model of pump dynamics developed here represents a fourth-order dynamics system that includes a second-order torque equilibrium equation of the yoke motion and two first-order continuity equations for the chamber volume of the yoke control cylinder and pressurized volume of pump and pipeline [7]. We will see that the pump dynamics have non-linearity due to the non-linear flow characteristics of the pressure compensator valve and load control valve. They are very complex due to the kinematics properties of the pumping mechanism [8] and the theoretical equation of pump dynamics under a proper sign rule are as follows. The flow continuity equation for the pressurized volume of pump and pipeline is [8]

$$\frac{1+\dfrac{\beta}{V_s}\dfrac{2\pi\left(\dfrac{d}{2}\right)^3 L(1-n^2)}{tE}}{\dfrac{\beta}{V_s}} P_s = Q_s - Q_l + Q_p' - C_2 P_s \qquad (1)$$

Where,

$$Q_s = 2R_1 \tan\theta A_1 N \frac{\omega}{2\pi} \qquad (2)$$

$$Q_l = C_d g_2 x_l \left\{\frac{2(P_s - P_o)}{\rho}\right\}^{1/2} \qquad (3)$$

$$Q_p' = \begin{cases} 0 & for \quad x_c \geq 0 \\ C_d g_1 x_c \left\{\dfrac{2(P_s - P_p)}{\rho}\right\}^{1/2} & for \quad x_c < 0 \end{cases} \qquad (4)$$

In the above equations, P_s is the outlet pressure of the pump, θ is the angular displacement of the yoke, Q_s is the outlet flow of the pump, Q_l is the load flow of the load control valve, Q_p' is the leakage flow due to the control flow of pressure compensator, x_l is the spool displacement of the load control valve, C_d is the discharge coefficient of orifice, g_1 and g_2 is the area gradient of orifice of pressure compensator and load control valve respectively, and x_c is the spool displacement of the pressure compensator.

The spool displacement x_c is written as

$$x_c = \frac{A_c(P_{sd} - P_s)}{k_c} \qquad (5)$$

Where P_{sd} is the desired value of the outlet pressure. In this relationship the dynamics of the spool motion are neglected. This is because the pressure compensator has a high stiffness spring and a small spool mass, resulting in much faster dynamics than the other dynamics of the pump system. In practice several previous researches [7, 8] have neglected the compensator dynamics in the pump dynamic model, and such models have been found to yield good agreement between experiments and computer simulation.

The torque equilibrium equation governing the angular yoke motion is

$$J\ddot{\theta}+\beta\dot{\theta}+(K_1d_1^2+K_2e^2)\tan\theta=(K_1d_1^2+K_2e^2)\theta_o-d_1A_1P_p+d_3A_3P_c+T....(6)$$

In this equation, θ is the angular displacement of the yoke, θ_o is the angular compression value of the yoke control spring at a yoke angle of 0 rad, k_1 and k_2 are spring coefficient, A_1 and A_3 are areas of the yoke control pistons and P_p is the pressure of the yoke control cylinder. T denotes the torque, which is caused by the pumping pistons rotating and reciprocating on the inclined yoke surface as shown in Fig.2.

The equation with regard to T is given by [7]:

$$T=\sum_{i=1}^{N}\frac{(-P_dA_2+M\omega^2R_1\tan\theta\sin\phi_i)(R_1\sin\phi_i+d_2\sin\theta-e)}{\cos^2\theta} \qquad (7)$$

Where, $\Phi_i=\phi+2\pi(i-1)/N$: i=1,2,3,.....N, and N is the number of pumping pistons. In this equation, P_d is the distributed pressure around the valve plate, M is the mass of the pumping piston, e is the eccentricity of the yoke pivot with respect to the barrel's axis, d_2 is the distance from the piston joint axis to the yoke pivot and ϕ_i is the angular position of the i^{th}-pumping piston. The flow continuity equation for the volume of the yoke control cylinder is

$$Q_p=A_1d_1\dot{\theta}/(\cos\theta)^2-C_1P_p+(V_o-A_1d_1\tan\theta)\dot{P}_p/\beta. \qquad ..(8)$$

$$Q_p=\begin{cases}C_d\cdot x_c\cdot g_1\sqrt{2(P_p-P_0)} & for \quad x_c\geq 0\\ C_d\cdot x_c\cdot g_1\sqrt{2(P_s-P_p)} & for \quad x_c<0\end{cases} \qquad (9)$$

In these equations, P_p is the pressure of the yoke control cylinder and Q_p is the control flow of the pressure compensator. In order to analyze easily the above complex dynamics, a model based on the state variable is more convenient. To derive the governing equations in a state variable form, the state variable vector x, input variable vector u and parameters veetor α will be defined:

$$x=[Ps,\ \theta,\dot{\theta},\ P_P]$$

$$u=[u_1,\ u_2]=\{P_{sd},\ c_1g_2x_1\ (2/p)^{1/2}\}$$

$$\alpha=[\alpha_1,\alpha_2,.....,\alpha_{13}]$$

In the above, the α_n vector consists of 13 parameter appearing in the governing equations and is listed in Table 3. Then the state equations become

$$\dot{x}_1=\{-\alpha_{12}x_1+\alpha_{10}x_2-u_2\sqrt{x_1}+R\alpha_1(u_1-x_1)\sqrt{Wx_1-Yx_4}\}/\alpha_{11}$$

$$\dot{x}_2=x_3.$$

$$\dot{x}_3=\{\alpha_7x_1-(\alpha_4-\alpha_{13})x_2-\alpha_3x_3-\alpha_6x_4-\alpha_4\alpha_5\}/\alpha_2$$

$$\dot{x}_4=\{\alpha_6x_3-\alpha_8x_4-\alpha_1(u_1-x_1)\sqrt{Wx_1-Yx_4}\}/\alpha_9 \qquad (10)$$

Where the auxiliary variables R, W, Y are variables to describe the non-linearity of the pressure compensator and are defined by

R=0 , W=0 , Y=-1 for $u_1\geq x_1$ (or $x_c\geq 0$)

R=1 , W=1 , Y=1 for $u_1<x_1$ (or $x_c<0$)

It is noted that equation (10) represents non-linear equations with 13 constant parameters. In the derivation of the state equations several assumptions were made, based upon consideration of the physical quantities of the variables associated with the pump dynamics. These include values of small yoke angle θ, constant value of V_o, small P_o and small d_2. In addition, torque T of equation (7) is averaged by

$$T = P_s \int_{-\pi/2}^{\pi/2} \frac{N}{2} \frac{A_2 e}{\pi} d\phi + \theta \int_0^{2\pi} NM\omega^2 R_1 \frac{\sin^2 \phi}{2\pi} d\phi \qquad \text{....(11)}$$

3- Dynamic Behavior, Results and Discussion

Using the Runge-Kutta fourth order method with step size Δt=0.4 ms, equations (10) are solved. Since the state variable of most interest is the outlet pressure P_s of the pump, the effect of different pipeline types with different lengths will be investigated with respect to this variable. The lengths of pipelines are chosen as 1,2,4,8 and10 meters with the sizes mentioned in Table 2.

Table 1. The geometrical and dynamic data of the pump system

A_c=3.019 x 10^{-5} m^2	A_1= 7.918 x 10^{-4} m^2
A_2= 2.85 x 10^{-4} m^2	A_3= 0.0
B = 9.5 x 10^{-2} Nms/rad	C_d =0.61
C_1= 7.03 x 10^{-6} m^3/MPas	C_2= 1.15 x 10^{-5} m^3/MPas
d_1= 5.6 x 10^{-2} m	d_2= 0.0 m
d_3= 0.0 m	e= 0.01 m
J =5.56 x 10^{-3} m^2 Kg	K_c= 6.84 x 10^4 N/m
K_1= 7.94 x 10^3 N/m	K_2= 1.53 x 10^4 N/m
g_1= 6.28 x 10^{-4} m	g_2= 1.22 x 10^{-4} m
M =9.0 x 10^{-2} kg	N=9
R_1= 3.73 x 10^{-2} m	V_o= 3.0 x 10^{-5} m^3
V_s= 1.7 x 10^{-3} m^3	β =680 Mpa (assumed)
P = 880 kg/m^3	ω = 183 rad/s
Θ_o = 1.03 rad	

Table 2 Pipeline characteristics

Material	E	ν	Size	ID	Thickness
Stainless-steel	193 GPa	0.28	-16	2.255 cm	0.1225 cm
			-24	3.75 cm	0.1625 cm
			-28	4.05 cm	0.1625 cm
			-32	4.675 cm	0.1625 cm
Aluminum-alloy	72.4 GPa	0.31	-16	2.255 cm	0.1225 cm
			-24	3.75 cm	0.1625 cm
			-28	4.05 cm	0.1625 cm
			-32	4.675 cm	0.1625 cm
Plastics (polystyrene)	4.2 GPa	0.41	-8	1.075 cm	0.0875 cm
			-10	1.387 cm	0.0875 cm
			-12	1.63 cm	1.225 cm
			-16	2.255 cm	1.225 cm
Reinforced plastic (Polyesters [glass-filled])	18 GPa	0.3	-8	1.075 cm	0.0875 cm
			-10	1.387 cm	0.0875 cm
			-12	1.63 cm	1.225 cm
			-16	2.255 cm	1.225 cm

Table 3. The constant parameters of the pump dynamic model

$\alpha_1 = (A_c / k_c) C_d g_1 (2/\rho)^{1/2}$	$\alpha_2' = J$
$\alpha_3 = \beta$	$\alpha_4 = k_1 d_1^2 + k_2 e^2$
$\alpha_5 = \theta_0$	
$\alpha_6 = A_1 d_1$	$\alpha_7 = \partial T / \partial P_s + A_3 d_3$
$= (N/2) A_2 e + A_3 d_3$	
$\alpha_8 = C_1$	$\alpha_9 = V_o / \beta$
$\alpha_{10} = 2 R_1 A_2 N (\omega / 2\pi)$	$\alpha_{11} = [1 + \beta / V_s (2\pi (d/2)^3 L (1-n^2) / t E] / (\beta / V_s)$
$\alpha_{12} = C_2$	$\alpha_{13} = \partial T / \partial \theta$
	$= N M \omega^2 R_1^2 / 2$

Figures.(4-10) show the effect of using Stainless-steel tubes on the outlet pressure against the time for two step cases, step decrease load flow and step increase load flow. The change in Overshoot percentage (OS%) and the equivalent natural frequency (ω_n) due the change of stainless steel tube's size and length in case of step decrease load flow are plotted in figures(9&10). Figures 11 and 12 show the changing of Undershoot percentage (US%) and the equivalent natural frequency (ω_n) due the change of Stainless steel tube's size and length in case of step increase load flow.

Figures (13 -17) show the effect of using Aluminum alloy tubes in the two step cases on the outlet pressure against the time. Figures 18 and 19 show the change of Overshoot percentage (OS%) and the equivalent natural frequency (ω_n) due the change of Aluminum alloy tube's size and length in case of step decrease load flow and Figs.20 and 21 in case of step increase load flow.

The effect of using plastic hoses on the pump dynamic characteristic (outlet pressure P_s) is shown in Figures (22-26). Figures 27 and 28 show the effect of these hoses on the Overshoot percentage (OS%) and the equivalent natural frequency (ω_n) in case of step decrease load flow. The effect on the Undershoot percentage (US%) and the equivalent natural frequency (ω_n) due the change of Plastic hose's size and length in case of step increase load flow is shown in Figures 29 and 30.

Finally, The effeet of using Reinforced plastic hose on the pump dynamic characteristic (outlet pressure P_s) is shown in Figures.(31-35). The effect of these hoses on the Overshoot percentage (OS%) and the equivalent natural frequeney (ω_n) in case of step decrease load flow is shown in Figures 36 and 37. The effect on the Undershoot percentage (US%) and the equivalent natural frequency (ω_n) due the change of Reinforced plastic hose's size and length in case of step increase load flow is shown in Figures 38 and 39.

From the previous study we notice the following:

A- For Stainless-steel tubes, the Overshoot percentage (OS%), Undershoot percentage (US%) and the equivalent natural frequency (ω_n) [the dynamic characteristic of the pump] are improved as the tube size increased, and improved more and more as the tube length increased. It is notice also that the outlet pressure 'P_s' curves are shifted to the right as the tube length increased (i.e. the settling time will increase). Also a certain steady state error will appear at the step decrease load flow case, and a certain Overshoot will appear after the main Undershoot at the step increase load flow case when the tube length is 8 meters and 10 meters. These mean that this pump with its control can be used with stainless-steel tube with different sizes and lengths.

B- For Aluminum alloy tubes, the Overshoot pereentage (OS%), Undershoot percentage (US%) and the equivalent natural frequency (ω_n) [the dynamic characteristic of the

pump] are improved as the tube size increased, and improved more and more as the tube length increased like the Stainless-steel tube, but the outlet pressure 'P_s' curves are shifted to the right more than the steel case as the tube length increased (i.e. the settling time will increase more and more). The appearing of the steady state error in the first case and the overshoot in the second case begin at tube length equal 2 meters. and increased more at tube length equal 4 meters. When the tube length is 8 meters or more, the pump outlet pressure curves show that the pump will be settled at a time more than 1 second in case of step decreasc load flow, and more fluctuation through the step increase load flow. This means that a more robust control is needed to use this pump with Al. alloy tube with tube length 8 meters or more.

C- For Plastic (Polystyrene) hose" with a suitable hose size" , the change of the hose size and the hose length improve the pervious pump dynamic characteristics more than at solid tubes, and its size change is more effective than at the solid tubes(i.e. a certain steady state error in case of decrease load flow and a certain overshoot appears at hose length equal 1 meter and increases more and more until hose length equal 8 meters. At plastic hose equal to 10 meters the dynamics characteristics of outlet pressure curves changed completely at the second hose size (10). This means that this pump is not suitable for installation with plastic hose more than 8 meters,(i.e. another robust control is needed to use this pump with Plastic hose with hose length more than8 meters)

D- For Reinforced plastic (Polyesters 'glass-filled') hose, with a suitable hose size, improves the pump dynamic characteristics like the other plumbing tubes. This type of hoses provides more pump dynamic characteristics improvement than the plastic hose and Al. alloy tubes (i.e. the steady state error on the outlet pressure curve in the step decrease load flow, and the small overshoot appears in the step increase load flow begins at hose length 4m with the largest size, and increase as the hose length increases).

E- Finally, we see that the Stainless-steel tube with different tube size and length. Aluminum alloy tube with different size to a tube length equal 4 meters, or tube sizes 16, 24 with tube length 8 meters, or tube sizes 16 with tube length 10 meters can be used safely in this pump with its pressure compensator. The Plastic hose with the different size with hose length 1 meter can also be used with this pump, and hose size 8 only with other hose lengths, while reinforced plastic is more suitable than the plastic hose or Al. alloy tube.

4- Conclusions

1. Plumbing tubes or hoses affect the dynamic characteristics of the pump, by increasing its size or its length, the Overshoot/Undershoot pereentage and the equivalent natural frequencies are improved, but settling time is inereased because the outlet pressure curves are shifted to the right
2. As the plumbing tubes be more flexible, the simulation of the outlet pressure P_s curves show that the pump is suitable for these types of hose or not
3. The studying of the pump dynamics characteristics without taking the effect of the pipeline installation don't give a correct simulation for actual pump application, especially in the long length application like the aircraft hydraulic systems. The designer must decide upon the suitable choice of the hose/tube to avoid undesired dynamics.

References

[1] Johnston, DN and Drew, JE. "Measurement of positive displacement pump flow ripple". Proc. IMechE Part I, Journal of systems & control Engineering, Vol. 210, p. 65-74, (1996).

[2] Edge, KA, Boston, OP., Xiao, S., Longvill, MJ., and Burrows, CR., "Pressure pulsations in reciprocating pump piping systems. Part 2: Experimental investigations and model validation" Proc. IMechE Part I, Journal of systems & control Engineering, Vol. 211, p. 239-250, (1997).

[3] Kim, S. D., Cho, H. S. and Lee, C. O., "A parameter sensitivity analysis for the dynamic model of a variable displacement axial piston pump ", Proc. Instn. Mech. Engrs. Vol. 201 Noc 4 p.235-243 (1987).

[4] Ye, R. Z., "Kinematics of axial piston pumps with swash plate and hydrostatic bearings", Basic Fluid Power Res. J., 18(1),PP.77-85, (1985).

[5] Zeiger, G. and Akers, A., "Dynamic analysis of an axial piston pump swash-plate control", Proc. Instn. Mech. Engrs. Part C, 200(c_1), p. 49-58 (1986).

[6] Lin, S. I., Akers, A. and Zeiger, G., "The Effect of Oil Entrapment in Axial Piston Pumps", ASME G00282, p. 127-134 (1984).

[7] Abd El-Magid, W. "Robust control of axial piston pump, Ph.D, thesis, Faculty of Engineering at Shoubra, Zagazig University 2002.

[8] Kaliafetis, P., and Costopoulos, T.H., "Modeling and simulation of an Axial Piston Variable Displacement Pump with Pressure Control", Mechanism and Machine Theory, Vol. 30, No.4, p.599-612, (1995)

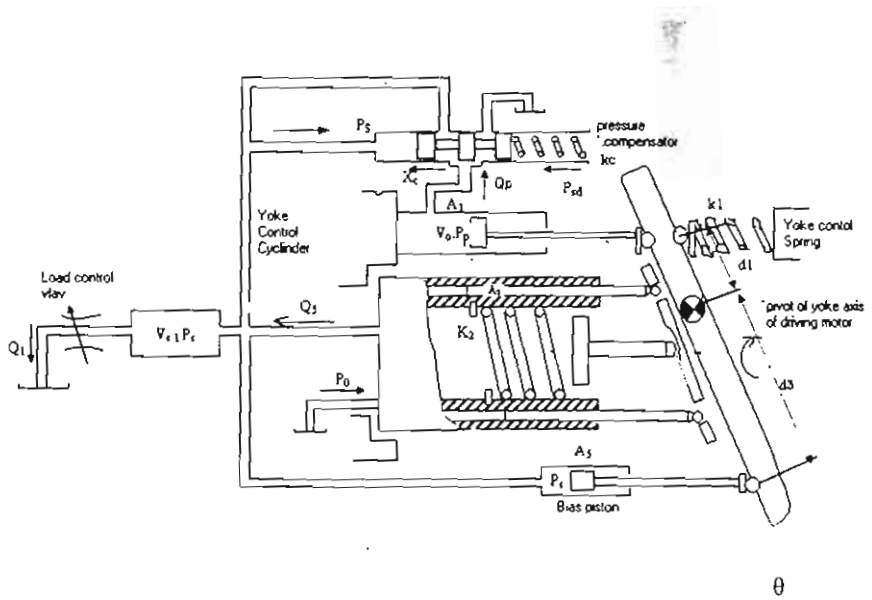

Fig.1. Structure of variable displacement axial piston pump

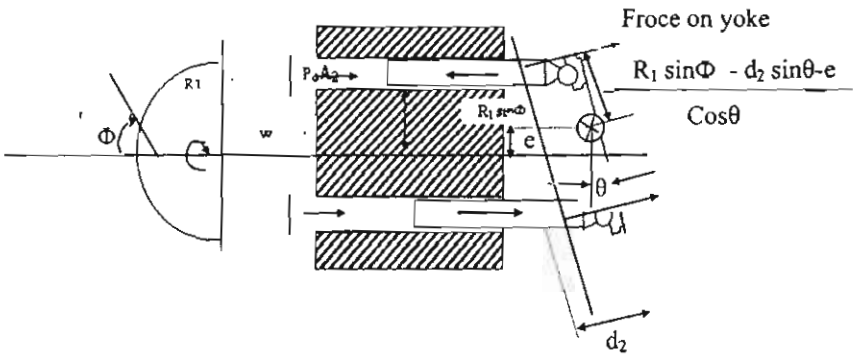

Fig.2. Kinematics diagram of pumping mechanism and reaction forces on the yoke

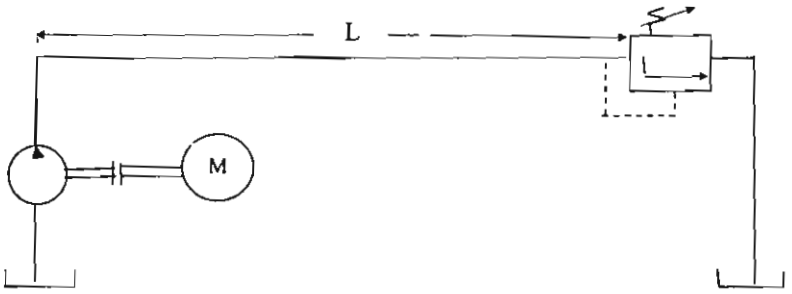

Fig.3 System under investigation

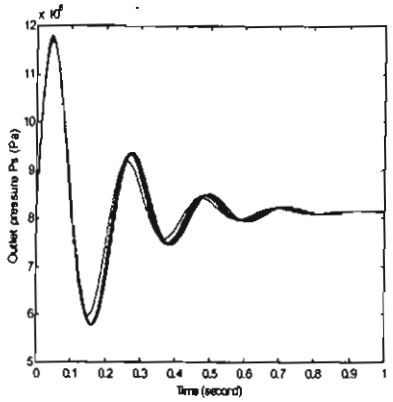

a) step decrease load flow

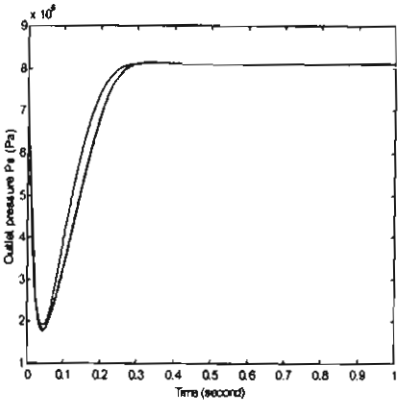

b) step increase load flow

Fig.4 Effect of using Stainless-steel tubes with length L=1 m

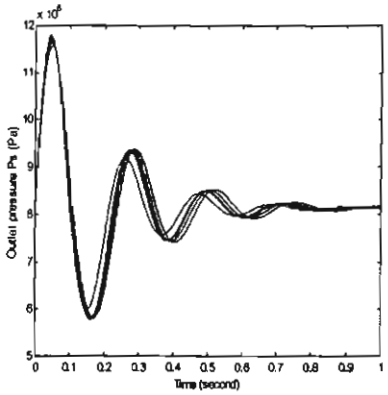

a) step decrease load flow

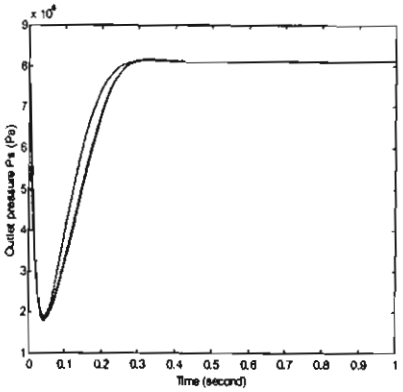

b) step increase load flow

Fig.5 Effect of using Stainless-steel tubes with length L=2 m

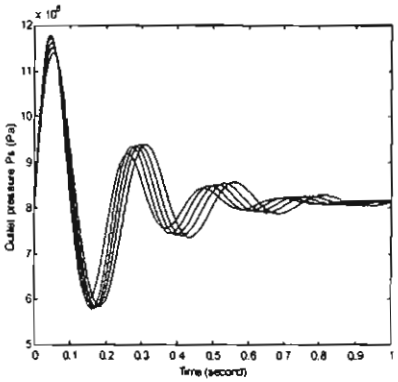

a)step decrease load flow

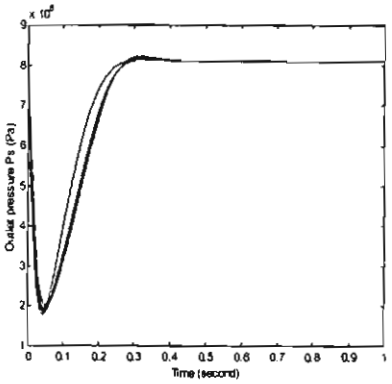

b) step increase load flow

Fig.6 Effect of using Stainless-steel tubes with length L= 4 m

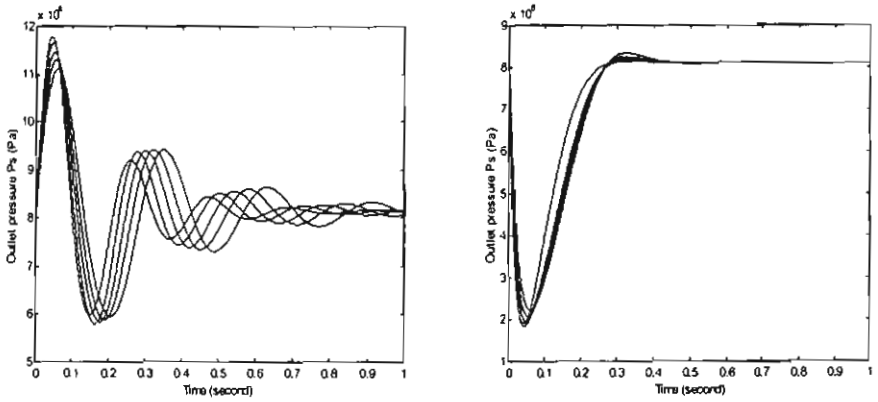

a)step decrease load flow b)step increase load flow

Fig.7 Effeet of using Stainless-steel tubes with length L= 8 m

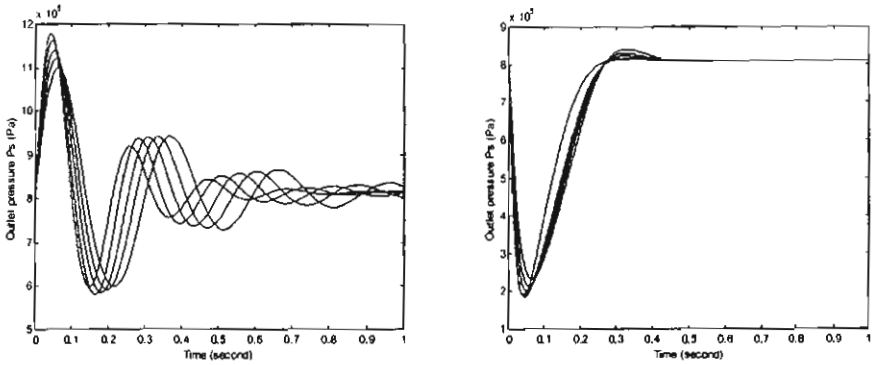

a)step decrease load flow b)step increase load flow

Fig.8 Effect of using Stainless-steel tubes with length L= 10 m

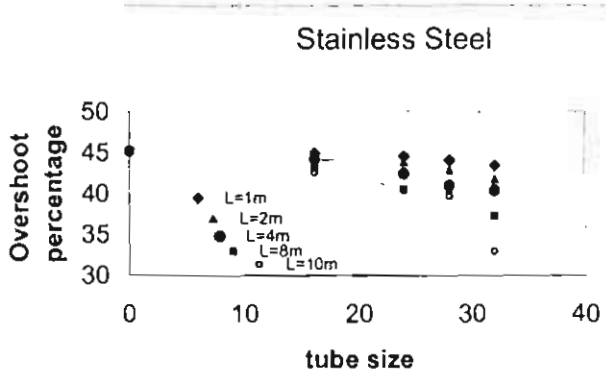

Fig.9 Effect of changing the Stainless steel tube size and length on OS% during step decrease load flow

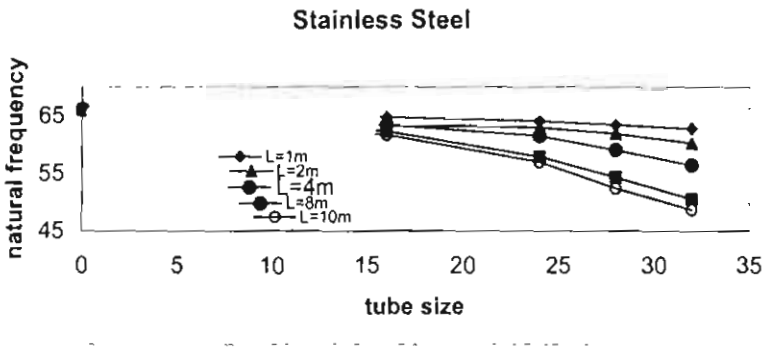

Fig.10 Effect of changing the Stainless steel tube size and length on ω_n during step decrease load flow

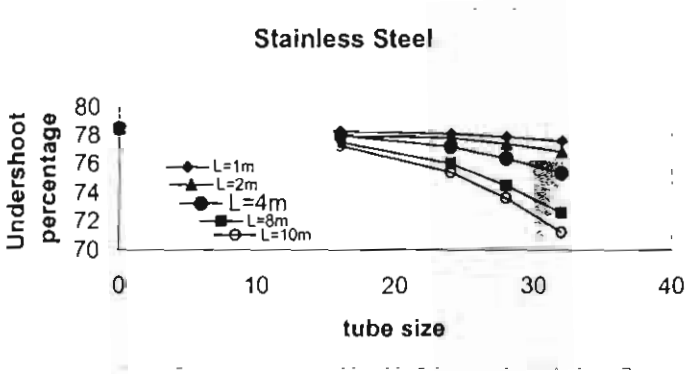

Fig.11 Effect of changing the Stainless steel tube size and length on OS% during step increase load flow

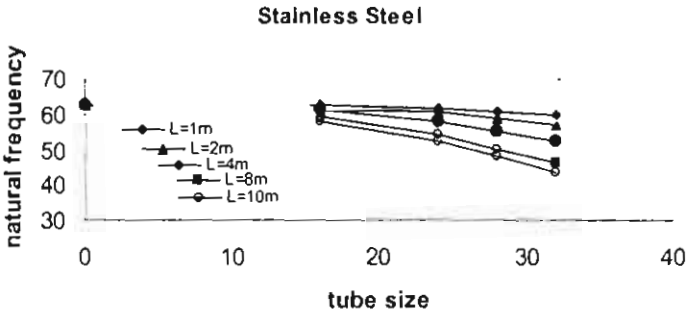

Fig.12 Effect of changing the Stainless steel tube size and length on ω_n during step increase load flow

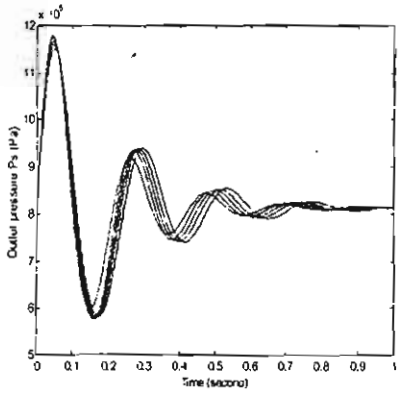

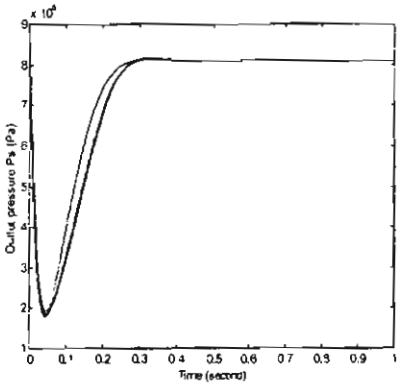

a)step decrease load flow b)step increase load flow

Fig.13 Effect of using Al. alloy tubes with length L=1 m

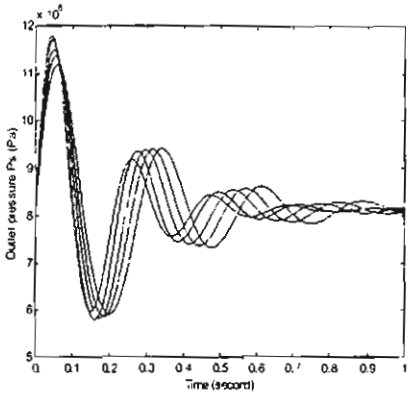

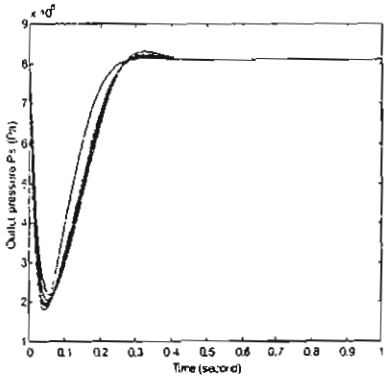

a)step decrease load flow b)step increase load flow

Fig.14 Effect of using Al. alloy tubes with length L=2 m

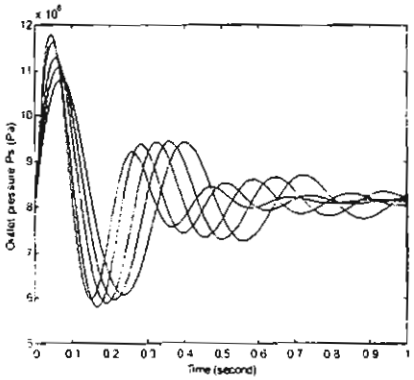

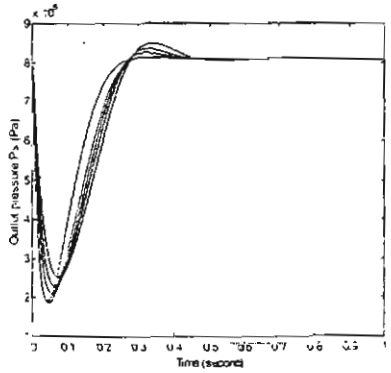

a)step decrease load flow b)step increase load flow

Fig.15 Effect of using Al. alloy tubes with length L= 4 m

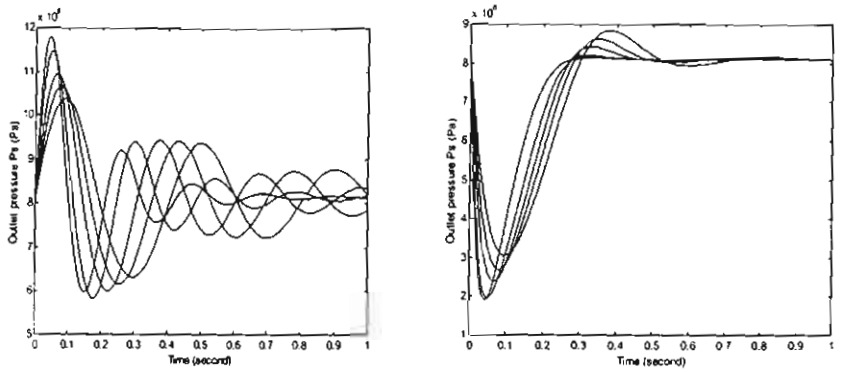

a)step decrease load flow b)step increase load flow

Fig.16 Effect of using Al. alloy tubes with length L=8 m

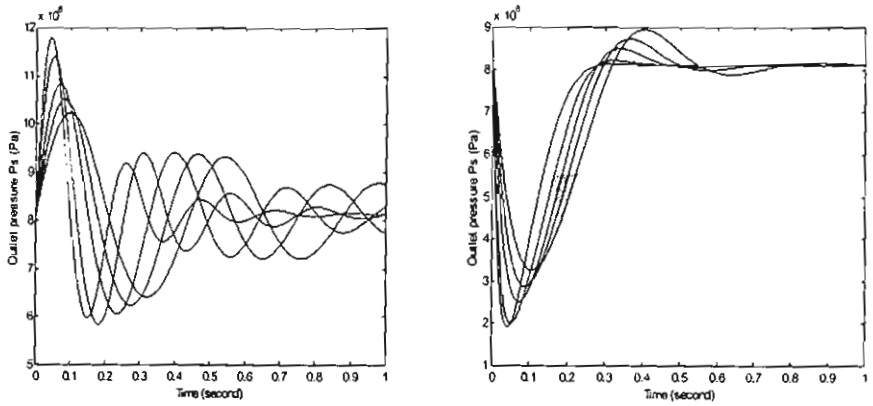

a)step decrease load flow b)step increase load flow

Fig.17 Effect of using Al. alloy tubes with length L=10 m

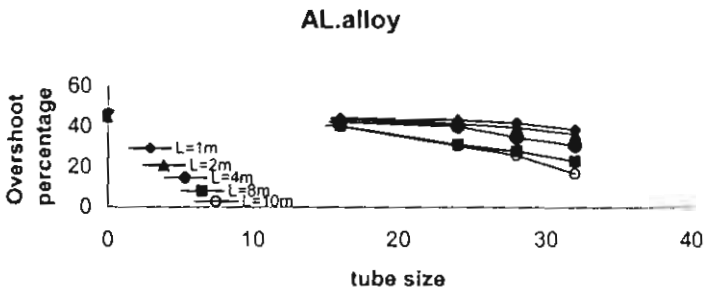

Fig.18 Effect of changing the Al.alloy tube size and length on OS% during step increase load flow

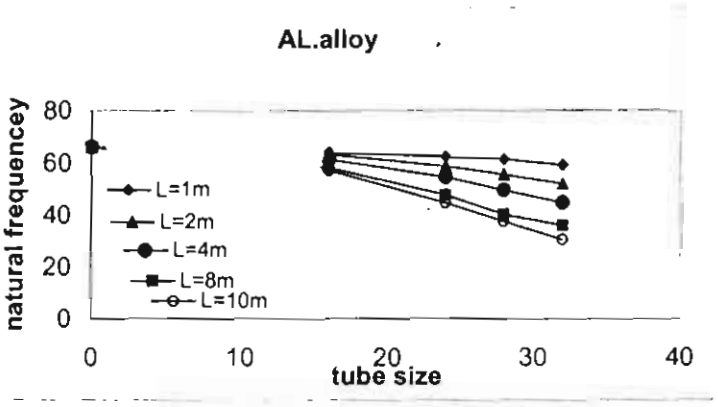

Fig.19 Effect of changing the Al.alloy tube size and length on ω_n during step decrease load flow

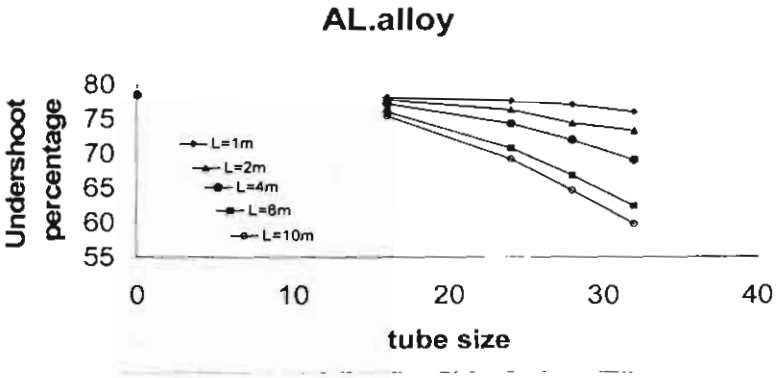

Fig.20 Effect of changing the Al.alloy tube size and length on US% during step increase load flow

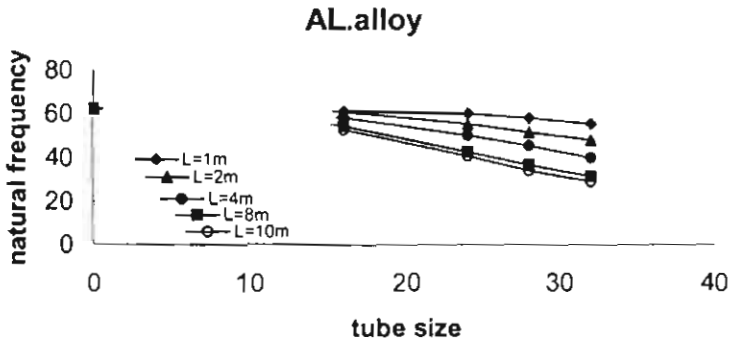

Fig.21 Effect of changing the Al.alloy tube size and length on ω_n during step increase load flow

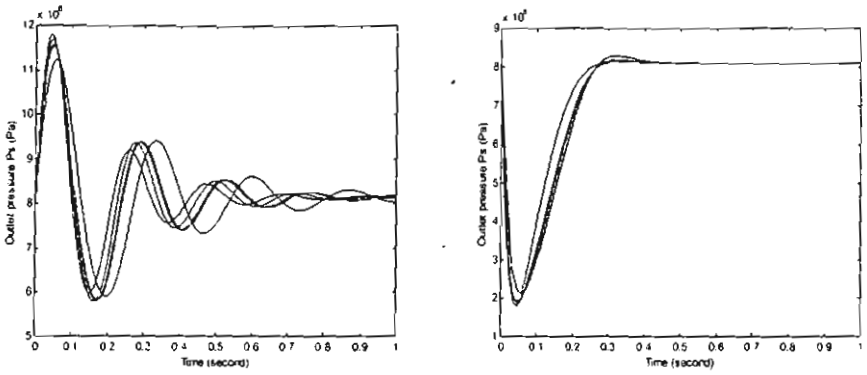

a)step decrease load flow b)step increase load flow

Fig.22 Effect of using Plastic hose with length L= 1 m

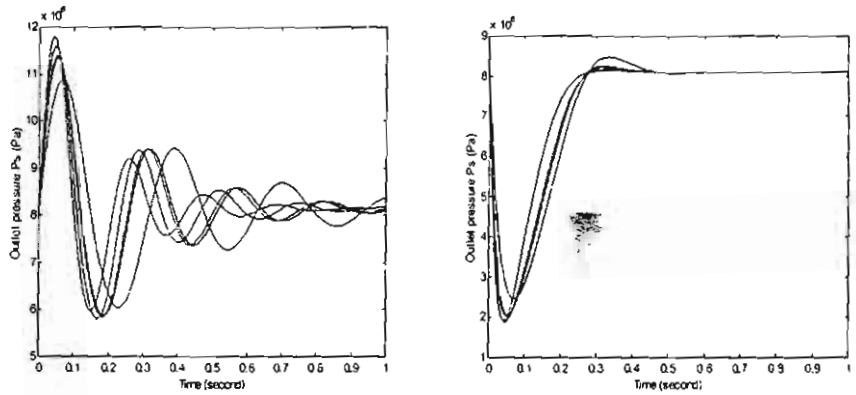

a)step decrease load flow b)step increase load flow

Fig.23 Effect of using Plastic hose with length L= 2 m

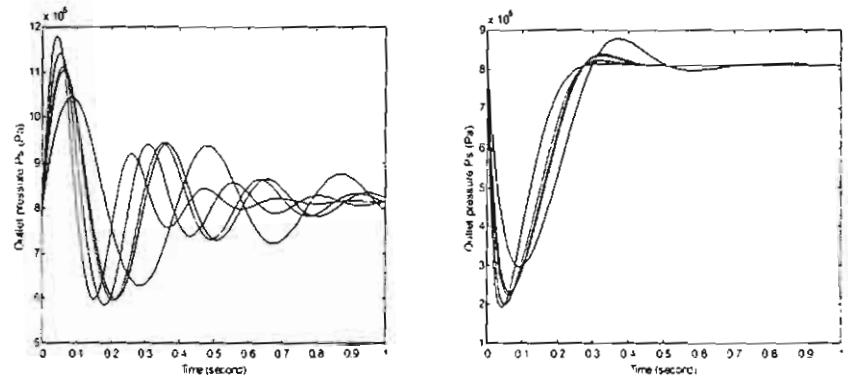

a)step decrease load flow b)step increase load flow

Fig.24 Effect of using Plastic hose with length L= 4 m

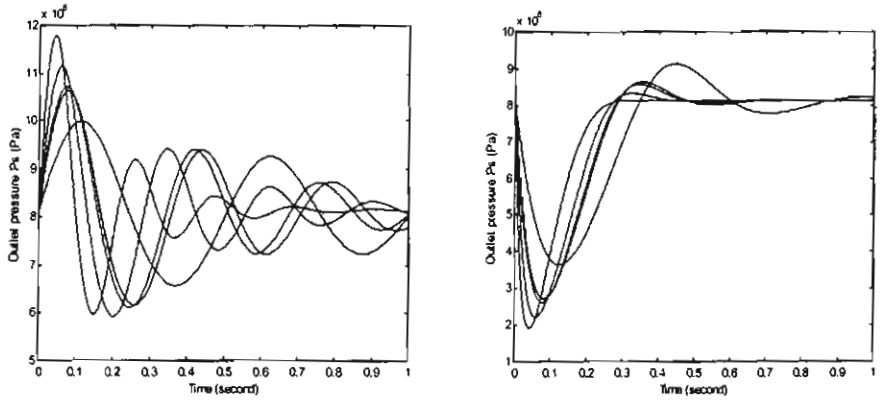

a)step decrease load flow b)step increase load flow

Fig.25 Effect of using Plastic hose with length L= 8 m

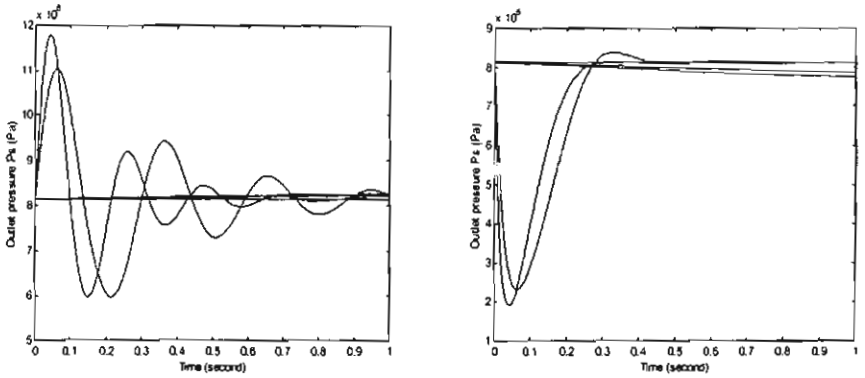

a)step decrease load flow b) step increase load flow

Fig.26 Effect of using Plastic hose with length L= 10 m

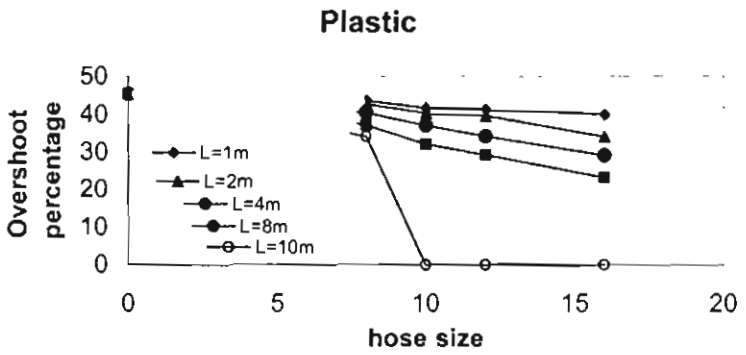

Fig.27 Effect of changing the Plastic hose size and length on OS% during step decrease load flow

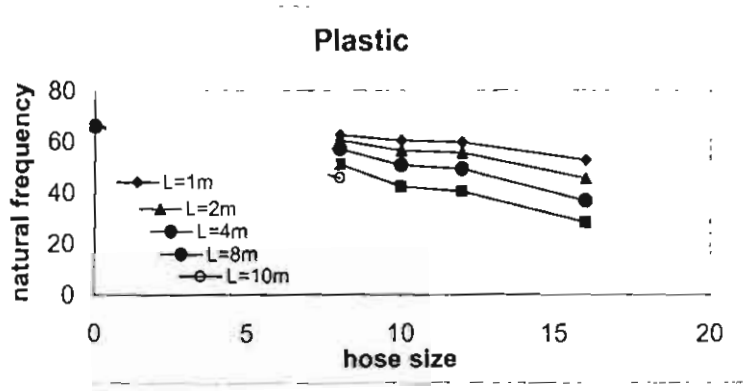

Fig.28 Effect of changing the Plastic hose size and length on ω_n during step decrease load flow

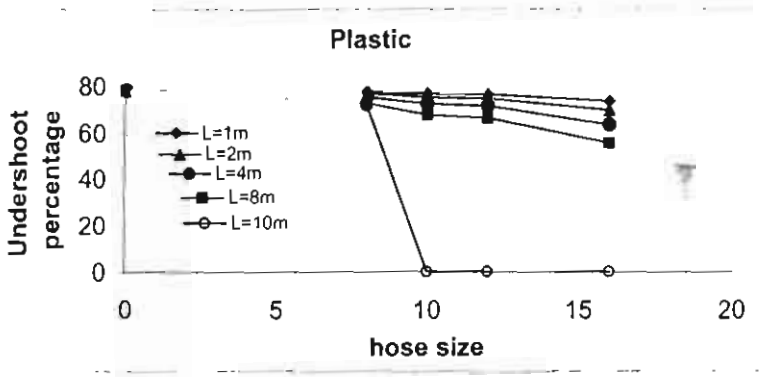

Fig.29 Effect of changing the Plastic hose size and length on US% during step increase load flow

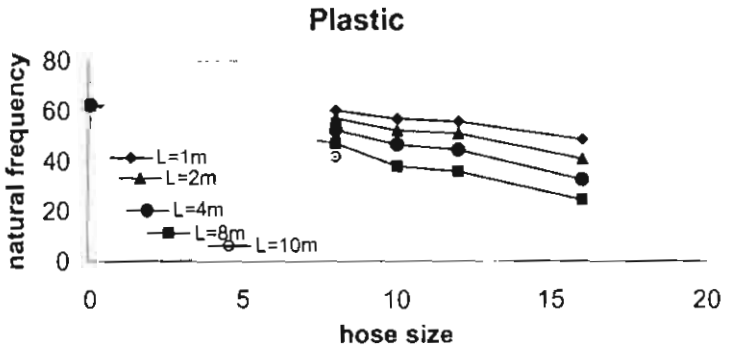

Fig.30 Effect of changing the Plastic hose size and length on ω_n during step increase load flow

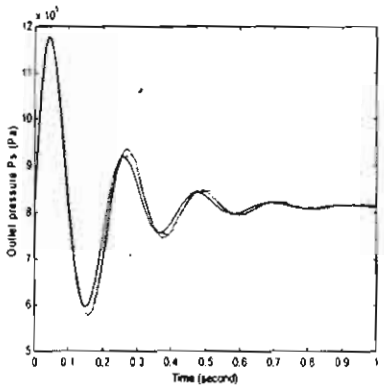

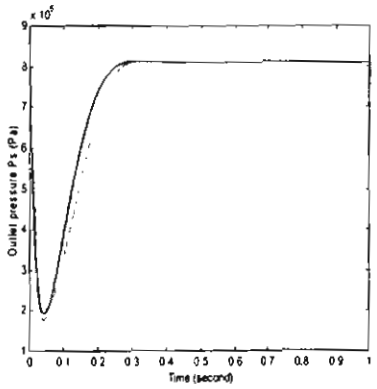

a)step decrease load flow b)step increase load flow

Fig.31 Effect of using reinforced plastic hose with length L= 1 m

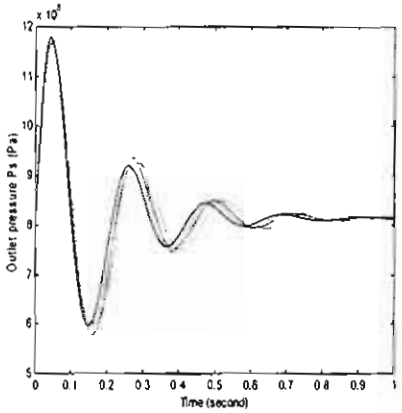

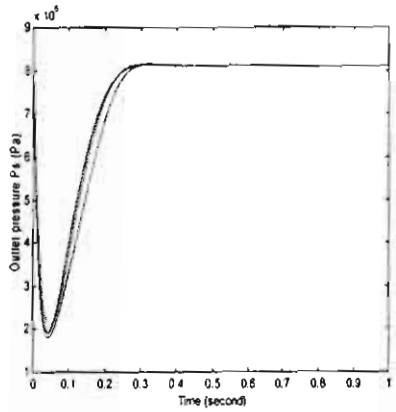

a)step decrease load flow b)step increase load flow

Fig.32 Effect of using reinforced plastic hose with length L= 2 m

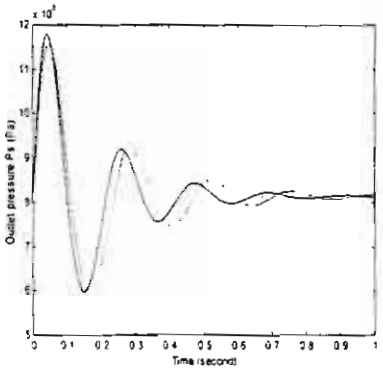

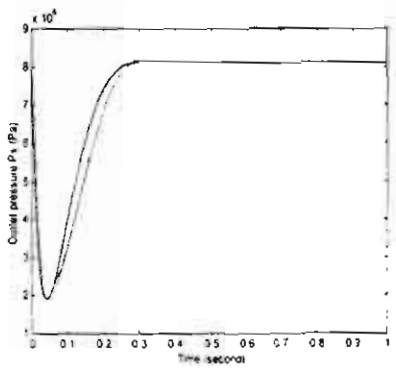

a)step decrease load flow b)step increase load flow

Fig.33 Effect of using reinforced plastic hose with length L= 4 m

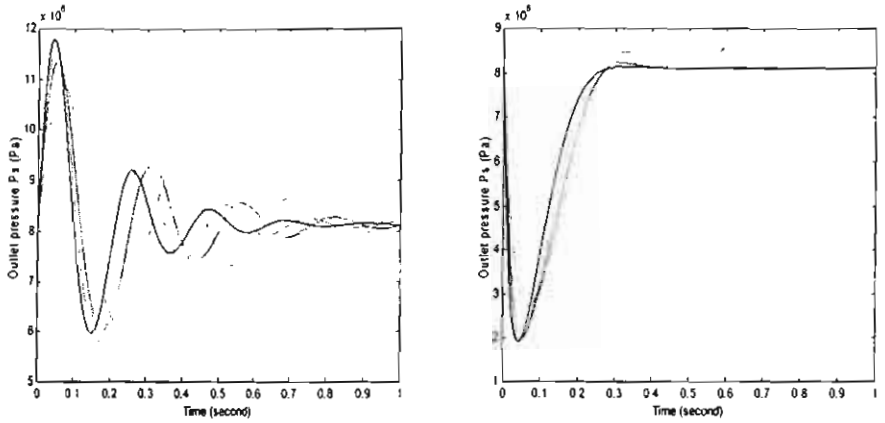

a)step decrease load flow b) step increase load flow

Fig.34 Effect of using reinforced plastic hose with length L=8 m

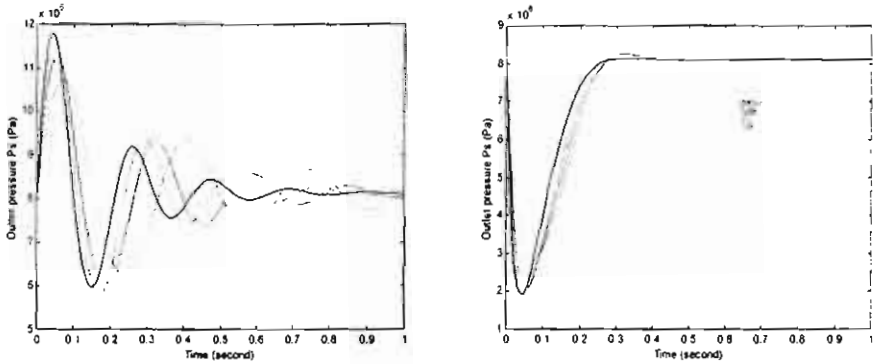

a)step decrease load flow b)step increase load flow

Fig.35 Effect of using reinforced plastic hose with length L= 10 m

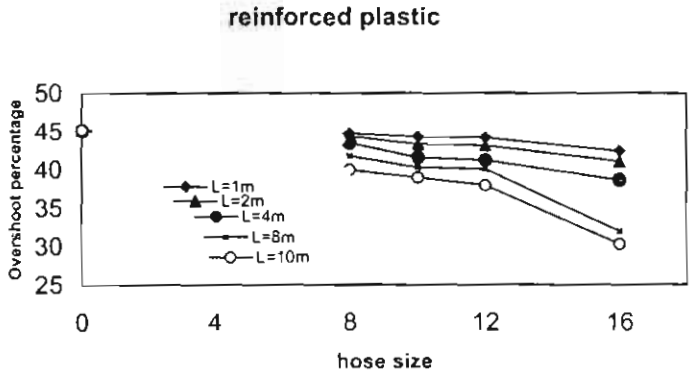

Fig.36 Effect of changing the reinforced plastic hose size and length on OS% during step decrease load flow

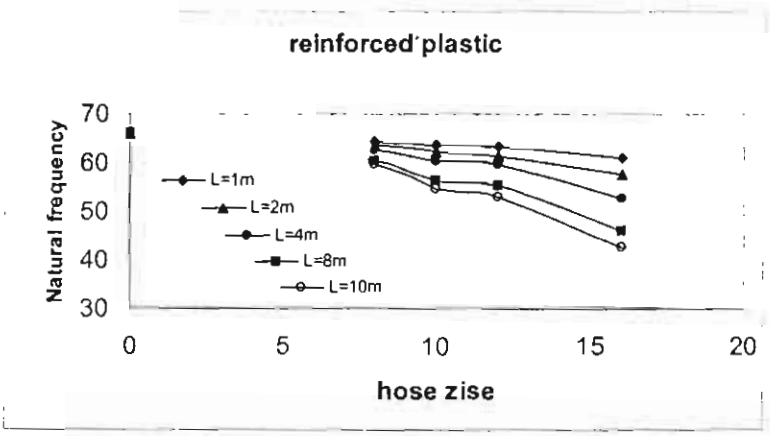

Fig.37 Effect of changing the reinforced plastic hose size and length on ω_n during step decrease load flow

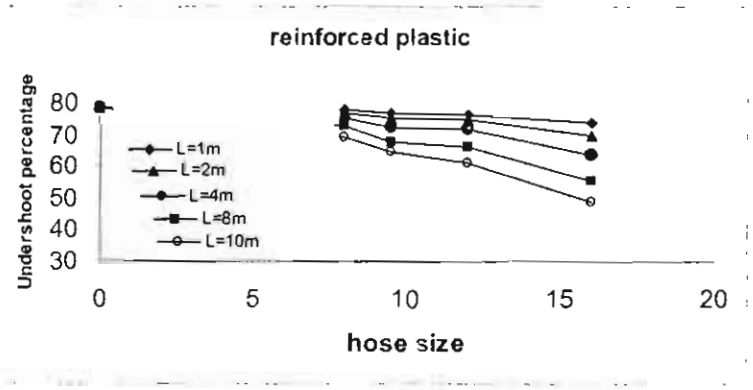

Fig.38 Effect of changing the reinforced plastic hose size and length on US% during step decrease load flow

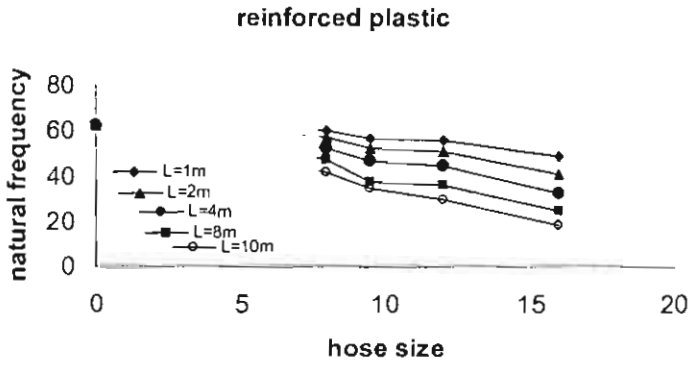

Fig.39 Effect of changing the reinforced plastic hose size and length on ω_n during step decrease load flow